

Spectroscopy of the stellar wind in the Cygnus X-1 system

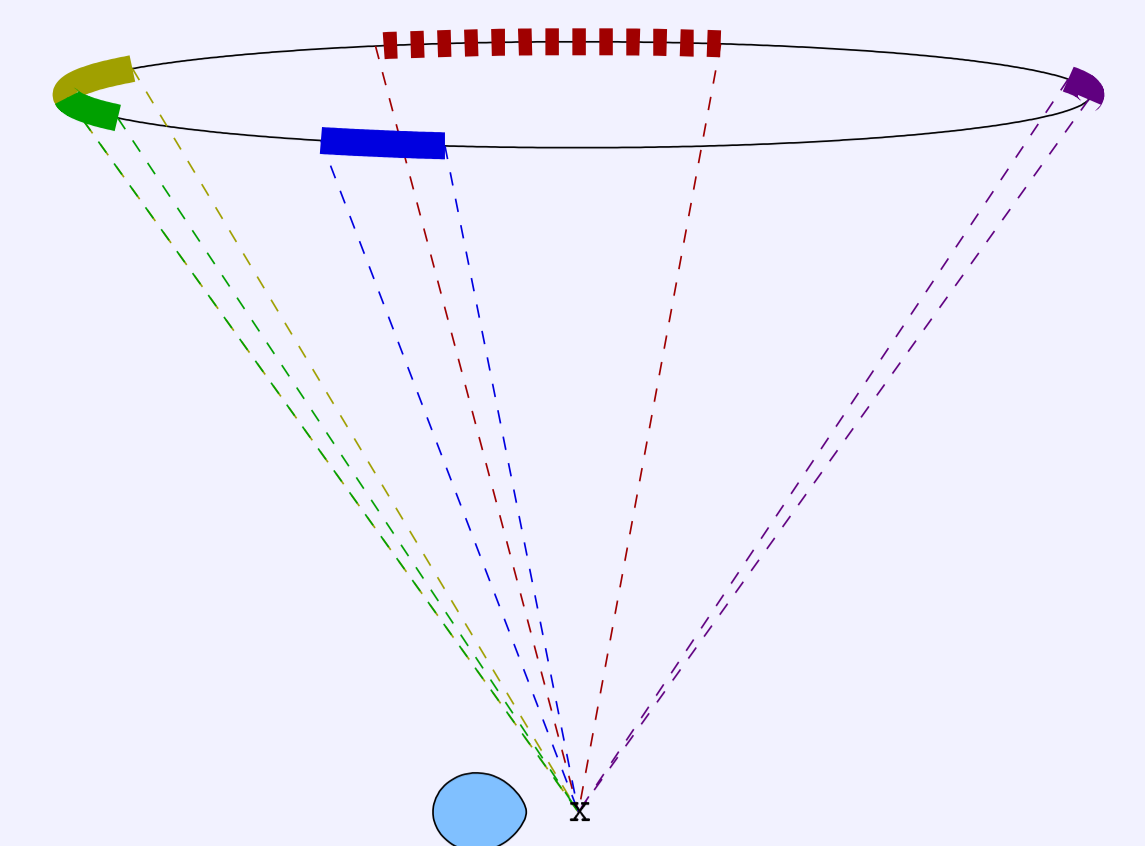
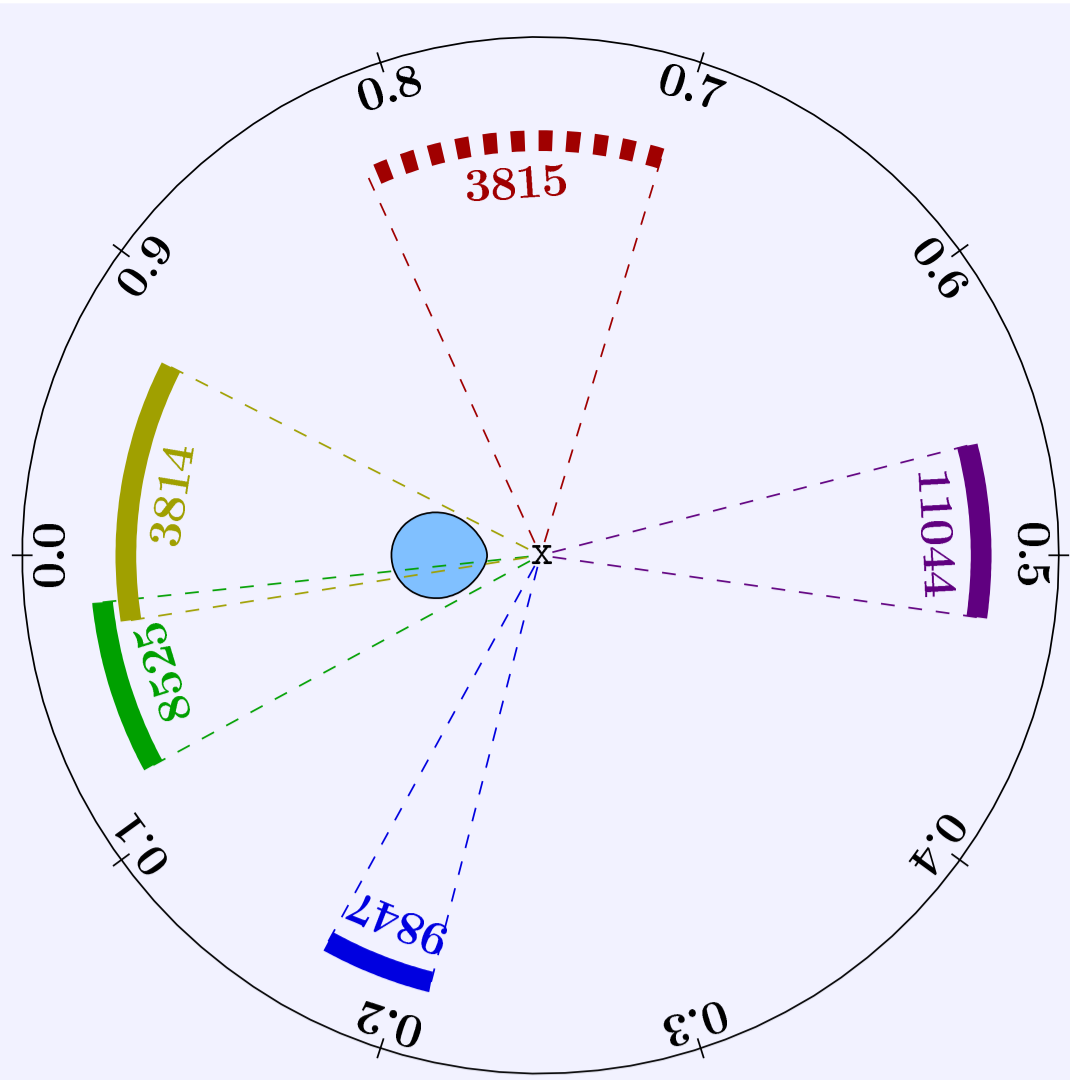
Ivica Miskovicova¹, Manfred Hanke¹

{Ivica.Miskovicova, Manfred.Hanke}@sternwarte.uni-erlangen.de

Jörn Wilms¹, Michael A. Nowak², Katja Pottschmidt³, Norbert S. Schulz²

¹ Remeis-Observatory / ECAP, University of Erlangen-Nuremberg, Germany

² MIT / Chandra X-ray Center, Cambridge (MA), USA ³ CRESST-UMBC/NASA-GSFC, Greenbelt (MD), USA



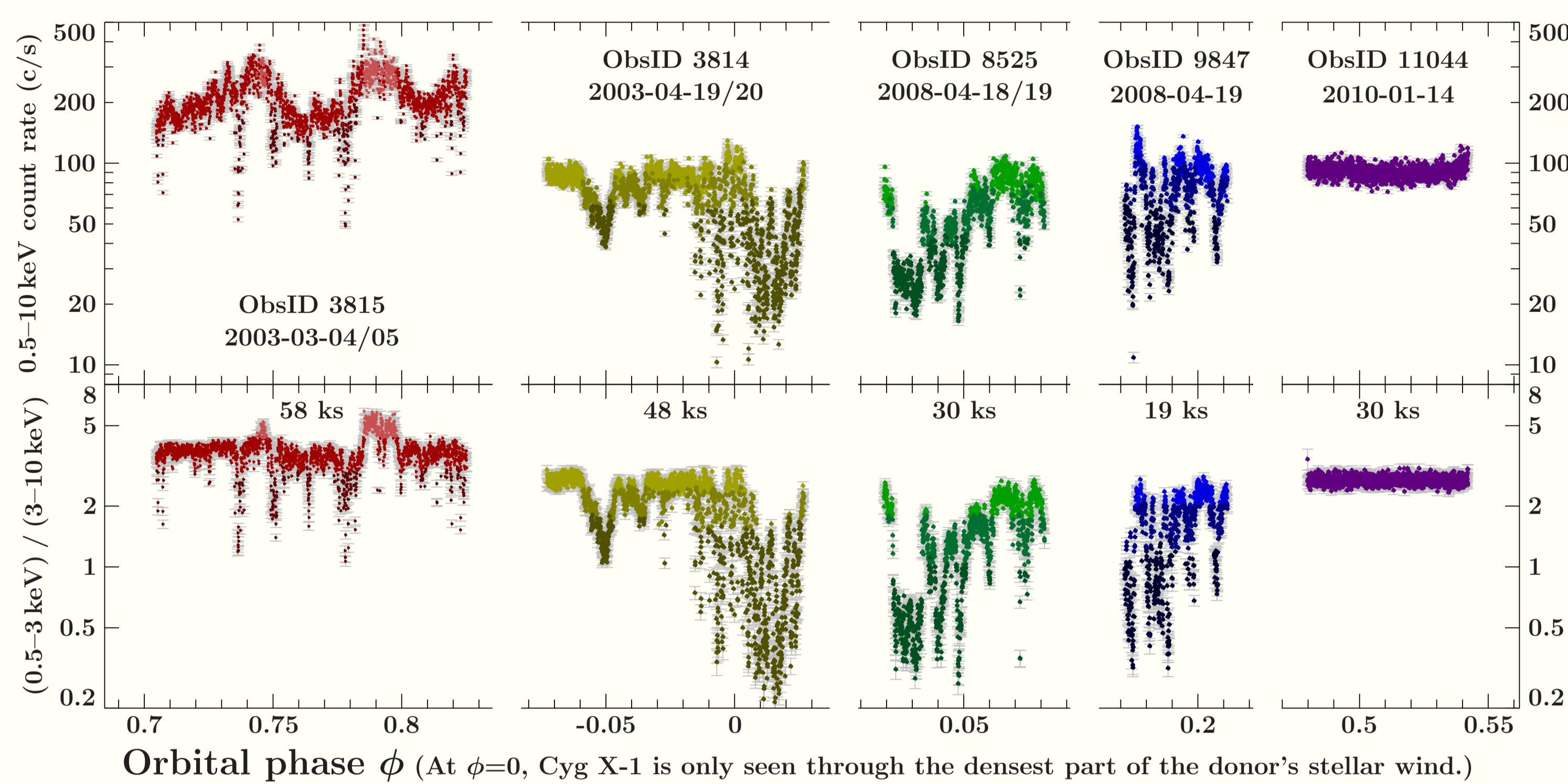
Abstract

The black hole high-mass X-ray binary Cygnus X-1 is powered by accretion of the stellar wind of its supergiant companion star HDE 226868. As the donor is close to filling its Roche lobe, its wind is therefore not symmetric, but strongly focused towards the black hole.

Chandra-HETGS observations allow for an investigation of this wind's properties. In the hard state, absorption lines of H- and He-like atoms reveal a highly photoionized wind. As different parts of the wind can be probed at different orbital phases of the binary system, we investigate the structure and dynamics of the wind by

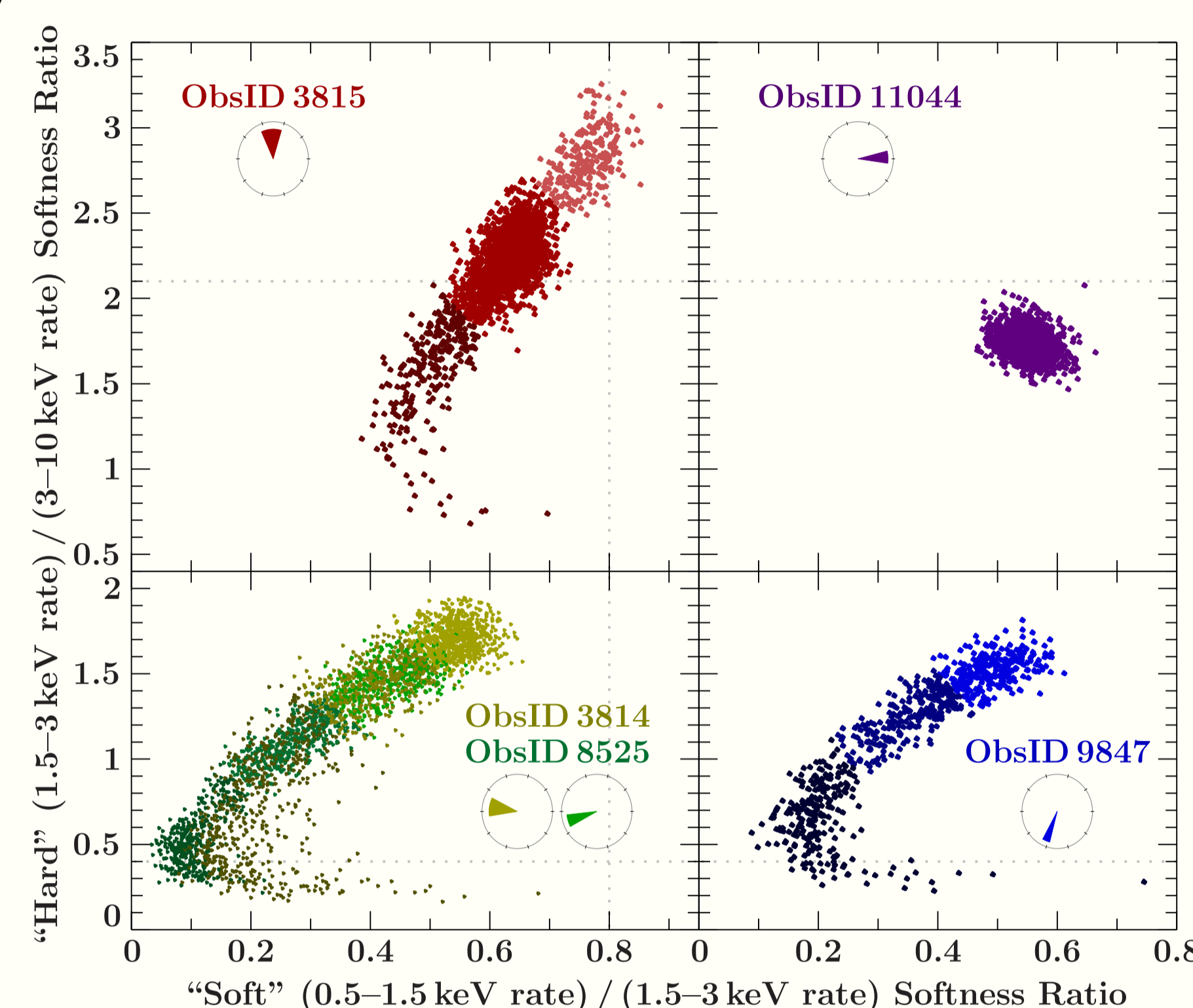
comparing observations at the prominent orbital phases $\phi=0, 0.2, 0.5,$ and 0.75 . In addition, we study transient dips. During these absorption events, caused by density inhomogeneities in the wind, lower ionization stages are detected.

Chandra observations around $\phi \approx 0.76, -0.02, 0.05, 0.19,$ and 0.51



While all recent Chandra observations caught Cyg X-1 in the hard state at $\lesssim 100$ c/s, comparable to ObsID 3814, the spectrum was softer and the flux was more than twice as high during ObsID 3815. The light curves at $\phi \approx 0$ are shaped by violent absorption dips, but dipping occurs already at $\phi \approx 0.7$ and has not ceased at $\phi \approx 0.2$, though the dip events seem to become shorter with distance from $\phi=0$. ObsID 11044 at $\phi \approx 0.5$ is totally free of dips, yielding 30 ks of remarkably constant flux.

Color-color diagrams reveal dips with partial covering



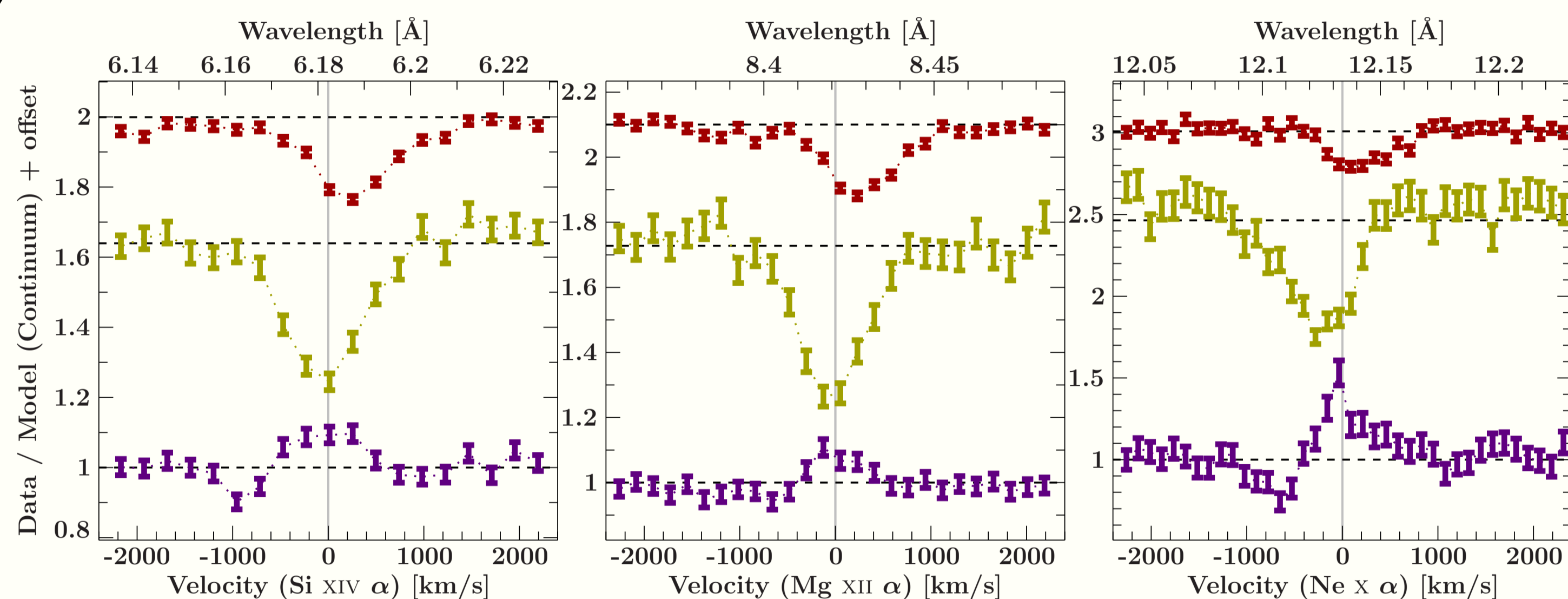
All of these diagrams show a "soft softness ratio" on the x - and a "hard softness ratio" on the y -axis.

Dipping produces a clear track in the color-color diagrams: At first, both colors harden towards the lower left corner, due to increased absorption. Then, during extreme dips, the soft color becomes softer again, indicating that the absorber causing the dips only partially covers the source of X-rays.

The apparent extraordinary softening after a flare in the CC-mode ObsID 3815 might be an instrumental artifact.

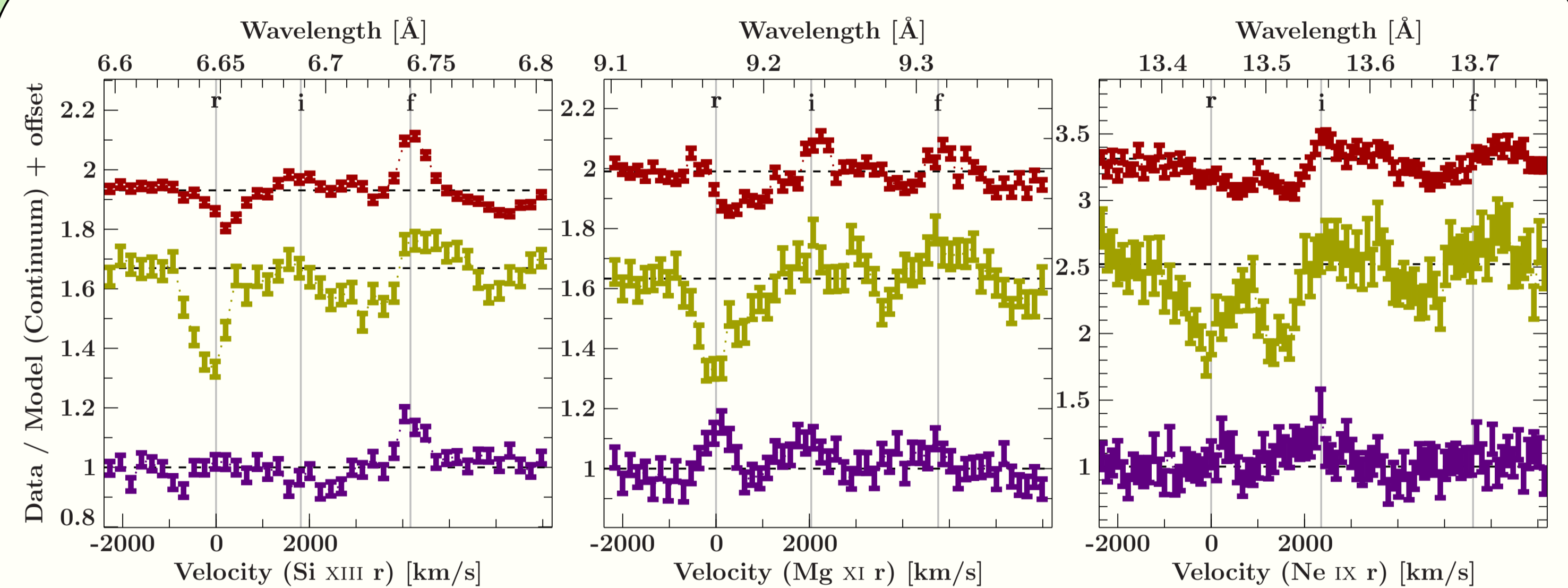
Different stages of dipping can be classified according to these softness ratios. In particular, we extract a "non-dip" spectrum from the least absorbed phases at the upper right corner (except for ObsID 3815). The following spectroscopic results refer to these non-dip phases.

Absorption and P Cygni line profiles of Lyman α transitions



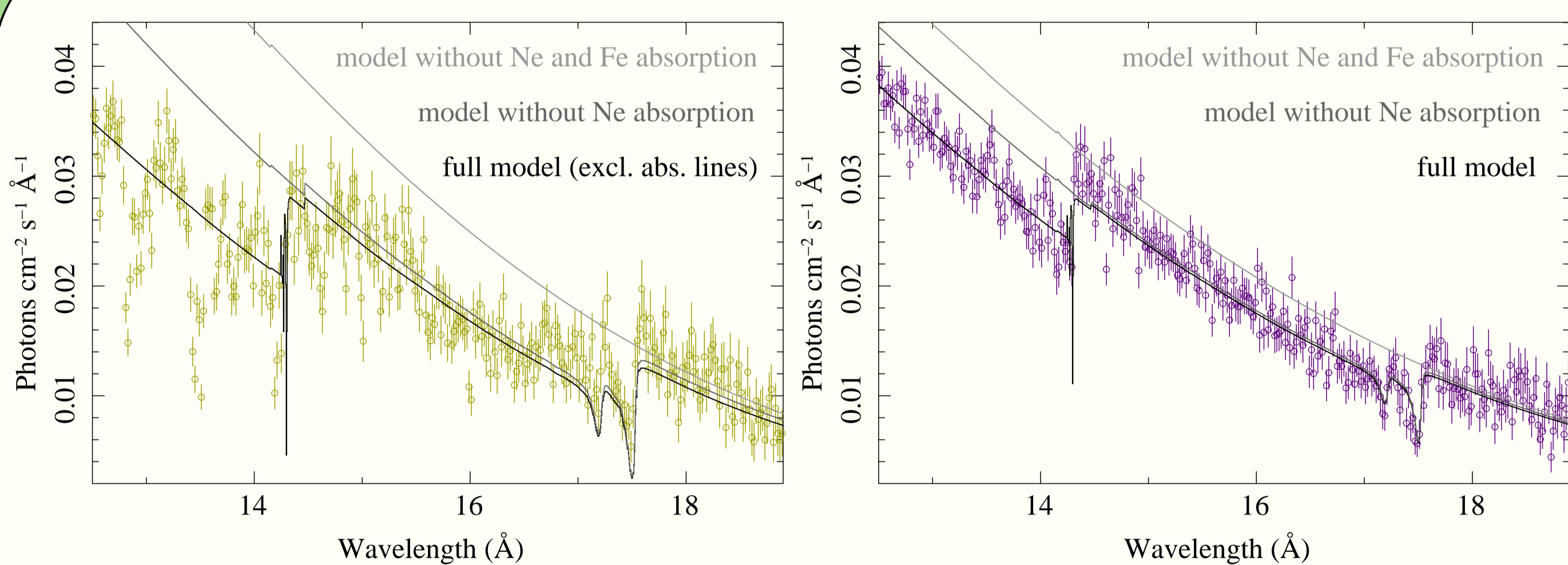
The highly photoionized wind is detected at $\phi \approx 0$ via numerous strong absorption lines at $v_{\text{rad}} \approx 0$. Lacking Doppler shifts can be explained by the wind flow being orthogonal to the line of sight (Hanke et al., 2008, 2009). However, the recent observation at $\phi \approx 0.5$ reveals (for the first time for Cyg X-1) clear P Cygni profiles with a strong emission component at a projected velocity $v_{\text{rad}} \approx 0$. If, despite the rotated line of sight by $2i \approx 70^\circ$, the emission at $\phi=0.5$ is caused by the same plasma as the absorption at $\phi=0$, its full space velocity must be quite small, i.e., we are probing a dense, low-velocity wind near the stellar surface. In contrast, the (relatively weak) absorption components at $\phi \approx 0.5$, occurring at a blueshift of ≈ 500 – 1000 km/s, demonstrate the downstream acceleration of the wind. The fact that the absorption line profiles measured at $\phi \approx 0.76$ are redshifted by ≈ 200 – 300 km/s proves that the wind flow is not radial from the star.

Comparison of He-like triplets



The $1s2s/1s2p \rightarrow 1s^2$ transitions of an He-like ion form the triplet of resonance, intercombination and forbidden lines, which can provide density and temperature diagnostics of an emitting plasma. In the observations at $\phi \approx 0.76$ and $\phi \approx 0$, the dipole-allowed r transition is, however, seen in absorption. (Note that the strong absorption ≈ 1500 km/s redward of Ne IX r is caused by Fe XIX.) Hanke et al. (2009) investigate the Mg XI i and f lines in the non-dip spectrum of ObsID 3814, which apparently consist of two pairs: one unshifted (consistent with other absorption lines), and one redshifted, from a denser plasma (with lower $R=f/i$ ratio), attributed to the focused wind. However, such a double pair is not clearly seen in the other spectra. While ObsID 11044 at $\phi \approx 0.5$ displays P Cygni-shaped Ly α lines, only the (weak) blueshifted absorption component from the Si XIII r transition, and only the (strong) unshifted emission component from Mg XI r are detected.

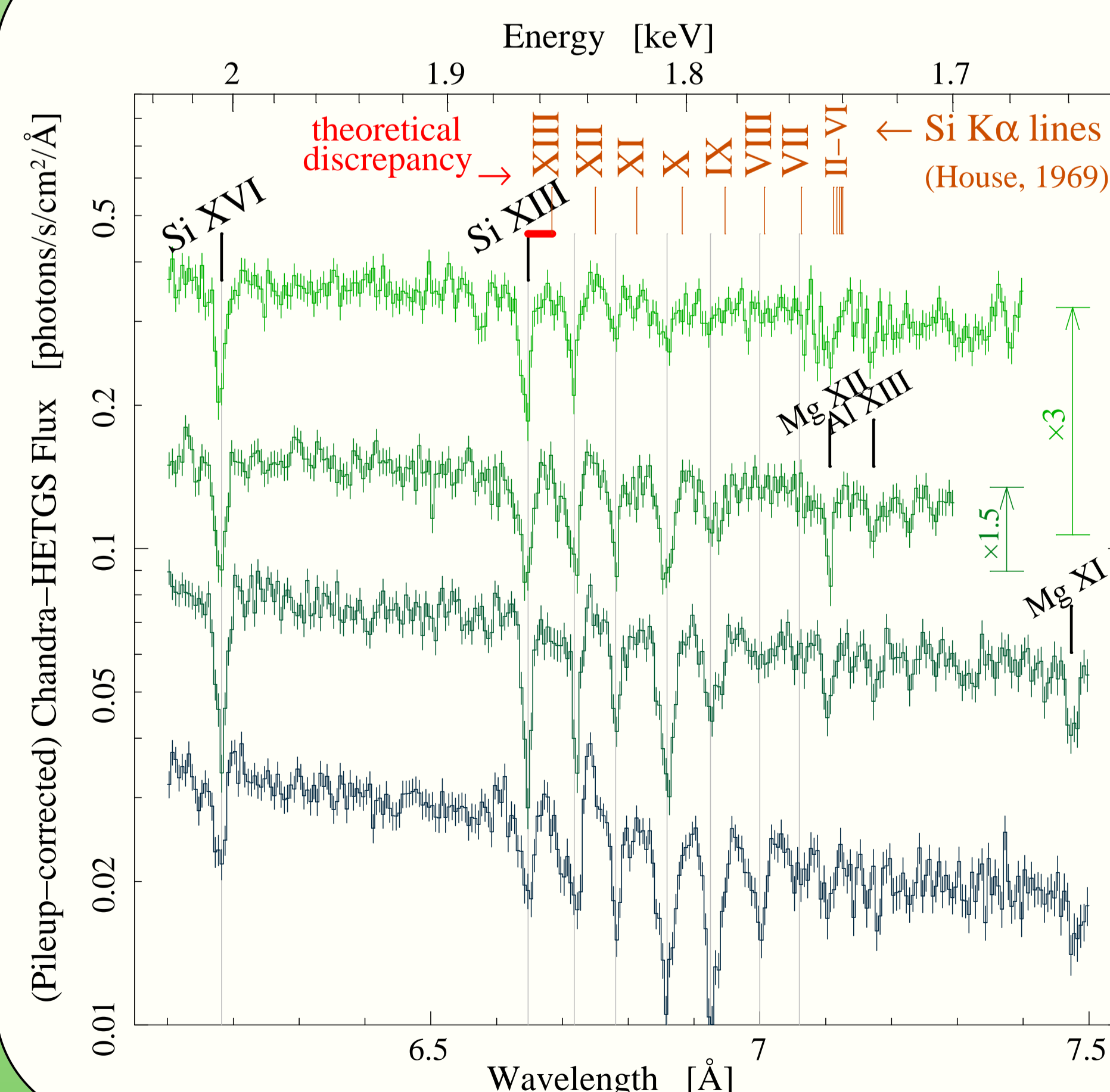
Neutral absorption: more indications for the wind?



While the 0.66–1 keV (non-dip) spectrum at $\phi \approx 0$ is dominated by complex Fe L-shell absorption (left: ObsID 3814), the most prominent features at $\phi \approx 0.5$ are neutral absorption edges, specifically the Ne K-edge at 14.3 \AA and the Fe L_2 and L_3 edges at 17.2 \AA and 17.5 \AA . The fine structures at these edges are taken into account by the tbnew model[†]. An accurate measurement of the neutral column density requires a good modelling of the continuum, which is complicated at $\phi \approx 0$ due to the large number of (probably unresolved) absorption lines. The preliminary fits shown above imply $N_{\text{Ne}} = 1.1 \times 10^{18} \text{ cm}^{-2}$ and $N_{\text{Fe}} = 2.8 \times 10^{17} \text{ cm}^{-2}$ at $\phi \approx 0$, but only $N_{\text{Ne}} = 5.6 \times 10^{17} \text{ cm}^{-2}$ and $N_{\text{Fe}} = 1.3 \times 10^{17} \text{ cm}^{-2}$ at $\phi \approx 0.5$.

[†] tbnew is an improved version of tb[var]abs (Wilms et al., in prep.). It uses internal caching of cross-sections and therefore performs much faster than many previous absorption models. One can fit relative abundances or total atomic column densities. The code is available at <http://pulsar.sternwarte.uni-erlangen.de/wilms/research/tbabs/>.

Low ionization stages from a cool(er) absorber during dips



ObsID 8525 was split into four parts according to the stage of dipping.

The first two spectra, corresponding to almost no and to weak dipping only, have been shifted by a factor $\times 3$ and $\times 1.5$ in flux (arrows) for visual clarity. Further reduction in flux in the last two spectra is real and due to dips.

While absorption lines of Si XIV and Si XIII are already present in the non-dip spectrum, the dip spectra contain additional strong absorption lines that can be identified with $K\alpha$ transitions of lower ionized Si XII–VII. (Note the systematic discrepancy of "adjusted line positions" reported by House (1969).) The strength of the low-ionization lines increases with the degree of dipping, suggesting that the latter is related to high-density clumps at lower temperature.

References

- Hanke, M., Wilms, J., Nowak, M. A., Pottschmidt, K., Schulz, N. S., & Lee, J. C. 2009, ApJ, 690, 330
 Hanke, M., Wilms, J., Nowak, M. A., Schulz, N. S., Pottschmidt, K., Lee, J., & Böck, M. 2008, in Proc. VII Microquasar Workshop, 29

